

Microwave excitation of spin wave beams in thin ferromagnetic films

P. Gruszecki,* A. E. Serebryannikov, and M. Krawczyk†

Faculty of Physics, Adam Mickiewicz University in Poznań, Umultowska 85, Poznań, 61-614, Poland

W. Śmigaj

Simpleware Ltd., Bradninch Hall, Castle Street, Exeter, EX4 3PL, UK

We present an approach enabling generation of narrow spin wave beams in thin homogeneous ferromagnetic films. The main idea is to match the wave vector of the spin wave with that corresponding to the spectral maximum of the exciting microwave magnetic field only *locally*, in the region of space from which the beam should be launched. We show that this can be achieved with the aid of a properly designed coplanar waveguide transducer generating a nonuniform microwave magnetic field. The resulting two-dimensional spin wave beams obtained in micromagnetic simulations propagate over distances of several micrometers. The proposed approach requires neither inhomogeneity of the ferromagnetic film nor nonuniformity of the biasing magnetic field, and it can be generalized to yield multiple spin wave beams of different width at the same frequency. Other possible excitation scenarios and applications of spin wave beam magnonics are also discussed.

PACS numbers: 75.30.Ds, 84.40.-x, 75.40.Gb, 76.50.+g

Magnonics is an emerging field of research and technology [1] whose area of interest is spin wave (SW) dynamics. It is closely related to photonics, which deals with electromagnetic waves, and phononics, which is concerned with elastic waves. Generation [2, 3], transmission [4, 5], signal processing [6], amplification [7], and detection [8] of SWs are major subjects of study in magnonics. Basic components performing these operations in nano- and mesoscale have been recently demonstrated. However, their functionality and performance require significant improvement to make magnonic elements competitive (in terms of energy efficiency, throughput, etc.) with other kinds of integrated devices: electronic, photonic or acoustic [9, 10]. The theoretical underpinnings of magnonics also constitute a rich and still not fully explored research area. SW caloritronics [11], magnonics-spintronics [12], magnonic crystals [13], magnonic metamaterials [14], and Bose-Einstein condensates of magnons [15] are some of the topics whose investigations have been started in recent years.

The crucial milestone in modern photonics (both from the scientific and the technological perspective) was the development of efficient sources of coherent light beams: lasers. In magnonics, an efficient source of coherent SW beams is still not available, in spite of many attempts at its development. The caustic effect [16], nonlinear self-focusing of SWs [17, 18], and inhomogeneous internal magnetic field (the sum of all magnetic fields inside magnetic material) [19] are among the beam excitation mechanisms investigated to date. The first is limited to low frequencies, i.e., to magnetostatic SWs, which have a caustic dispersion relation. The excitation is limited to specific angles with respect to the direction of the magnetization vector, which needs to be in the plane of the film. The second approach requires excitation of SWs with high amplitude and the beam spreads quickly after

passing the focal point. In the third approach, it is necessary to create an inhomogeneity of the internal magnetic field, i.e., to enclose SW excitations to propagate within channels of the static magnetic field with decreased magnitude, thus technologically complex.

On the other hand, electromagnetic wave transducers—microstripe and coplanar waveguides (CPWs)—are extensively used in studies of SWs in thin ferromagnetic films [20, 21], in particular as sources of plane-wave-like SWs. In this paper, we propose and numerically validate with micromagnetic simulations (MSs) a method of excitation of narrow SW beams in homogeneous ferromagnetic thin films using the magnetic field generated by microwave-frequency transducers with a suitable geometry. We demonstrate that efficient excitation of a SW beam can occur only within those space regions where the wave vectors of the SW and the Fourier-transformed distribution of the microwave (mf) magnetic field match. To ensure that this condition holds only locally, we vary the transducer's profile along the current flow direction. This affects the spatial distribution of the magnetic field induced by the current and, in particular, its Fourier spectrum along the expected direction of SW propagation. In its most basic form, this method enables excitation of a single well-localised SW beam propagating perpendicularly to the waveguide axis. By adapting the transducer's geometry, this approach can be generalised so that multiple SW beams of identical or different width appear simultaneously in different regions of the ferromagnetic film. Other possible scenarios and applications are also discussed.

Throughout this paper, we consider the propagation of SWs in a ferromagnetic film of thickness $t_f = 20$ nm made of yttrium-iron garnet (YIG). YIG is a promising dielectric material with the lowest damping of SWs ever recorded. Recently, the technology of ultra-thin YIG

film deposition has been developed, holding promise for integrated magnonics [24, 25]. We assume the film is saturated normal to its plane, i.e., along the z axis, by an external magnetic field $\mu_0 H = 1$ T, where μ_0 is the permeability of vacuum. We take the YIG magnetization saturation to be $M_S = 0.194 \times 10^6$ A/m, exchange constant $A = 0.4 \times 10^{-11}$ J/m, and gyromagnetic ratio $\gamma = 176$ rad GHz/T [26].

The results of MSs reported in this paper have been obtained with the open-source software MuMax3 employing the finite difference method [23]. We used a finite difference grid with resolution 5 nm in the x and y directions (i.e., in the film plane) and 20 nm in the z direction (along the normal to the film surface) and the Landau-Lifshitz equation was solved using the RK45 (Dormand-Prince) method [27, 34]. The distributions of the magnetic fields generated by CPWs and used to excite the SWs have been calculated with CST Microwave Studio, a commercial Maxwell solver based on the finite integration method [22].

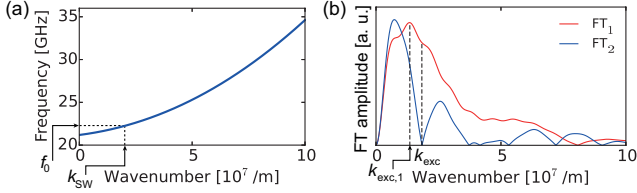


Figure 1. (a) The dispersion relation of SWs in a 20-nm thick YIG film with out-of-plane magnetization placed in an external magnetic field of 1 T. (b) The Fourier transforms FT_1 and FT_2 of the microwave magnetic fields $h_{y,1}^{mf}(y)$ and $h_{y,2}^{mf}(y)$ emitted by two CPWs, CPW₁ and CPW₂, at frequency f_0 . $k_{exc,1}$ is the location of the maximum of FT_1 . At $k_{exc} = k_{SW}(f_0)$, the wave number of SWs at frequency f_0 , the value of FT_1 is still close to maximal, while FT_2 has a minimum.

Let us now discuss the basic principle of the selective (local) wave vector matching. Following [8], we assume that the efficiency of monochromatic SW excitation by a CPW depends, in particular, on the quality of the match between the wave number $k_{SW}(f_0)$ of the SW at the excitation frequency $f = f_0$ and the wave number k_{exc} corresponding to the maximum of the Fourier transform (FT) of the microwave magnetic field \mathbf{h}^{mf} oscillating at the same frequency. Thus, the most efficient excitation of SWs occurs when

$$k_{SW}(f_0) = k_{exc}. \quad (1)$$

On the other hand, if the magnitude of the FT at a wave number $k = k_{nexc}$ is very small, there is no matching and no efficient SW excitation should arise. These facts make it possible to engineer the wavefronts of excited SWs, and in particular to excite SW beams with high efficiency.

Figure 1(a) shows the dispersion relation of SWs in a YIG film of thickness $t_f = 20$ nm, calculated with the analytical formula [26]

$$f(k_{SW}) = \frac{\gamma\mu_0}{2\pi} \left[\left(H - M_S + \frac{2A}{\mu_0 M_S} k_{SW}^2 \right) \times \left(H + \frac{2A}{\mu_0 M_S} k_{SW}^2 - M_S \frac{1 - e^{-k_{SW} t_f}}{k_{SW} t_f} \right) \right]^{\frac{1}{2}}. \quad (2)$$

In line with Eq. (2), the dispersion is independent from the direction of the wave vector and has a predominantly parabolic behavior in the considered wave number range.

For reasons discussed below, SWs are excited mainly by the microwave magnetic field component parallel to the expected direction of their propagation, further denoted by y . Thus, we focus on the behavior of $\mathcal{F}[h_y^{mf}(y)]$, the FT of $h_y^{mf}(y)$. Fig. 1(b) shows the Fourier transforms $FT_1 = \mathcal{F}[h_{y,1}^{mf}(y)]$ and $FT_2 = \mathcal{F}[h_{y,2}^{mf}(y)]$ of the magnetic fields generated by two realistic uniform transducers. Their geometry will be detailed later in the paper. At frequency $f_0 = 22.12$ GHz [29], Eq. (1) holds only for FT_1 [$k_{exc} = 1.8 \times 10^7 \text{ m}^{-1} \approx k_{SW}(f_0)$, see Fig. 1]; therefore one may expect that at this frequency SWs can be excited only with the field $h_{y,1}^{mf}(y)$. The transducer is designed so that it produces the magnetic field distribution $h_{y,2}^{mf}(y)$ over most of its length and $h_{y,1}^{mf}(y)$ only along a short section, an SW will be excited only in that short section of the transducer. Provided that this section is at least a few times longer than the SW wavelength, this should give rise to a well-collimated SW beam. Beam excitation in a wide frequency band will be possible if the dip in FT_2 near $k_{exc} = k_{SW}$ is sufficiently broad and the slope of the SW dispersion relation near k_{exc} sufficiently steep.

Now, let us briefly revisit SW excitation by the microwave magnetic field induced by a current flowing through the uniform transducer shown in Fig. 2(a) [21]. The CPW consists of a signal line of width w separated by gaps of width s from two identical ground lines. All lines are deposited on a nonmagnetic, dielectric layer of thickness t_d covering the ferromagnetic film. A microwave signal in the CPW generates the field \mathbf{h}^{mf} , which oscillates in the (y, z) plane, i.e., perpendicular to the CPW axis, see Fig. 2(b). In the plane of the ferromagnetic film, only the y component of this field exerts a non-zero torque on the magnetization, which is parallel to the z axis. This torque induces coherent magnetization precession around the equilibrium direction and causes generation of SWs propagating along the y axis.

Figure 2(c) shows the profile of the microwave magnetic field 7.5 nm below the ground and signal lines of two CPWs made of Cu with conductivity $\sigma = 5.88 \times 10^7$ S/m [30], nm, operating at $f_0 = 22.12$ GHz. The dielectric layer has thickness $t_d = 5$ nm. The width of the signal line in CPW₁ is $w_1 = 65$ nm and in CPW₂,

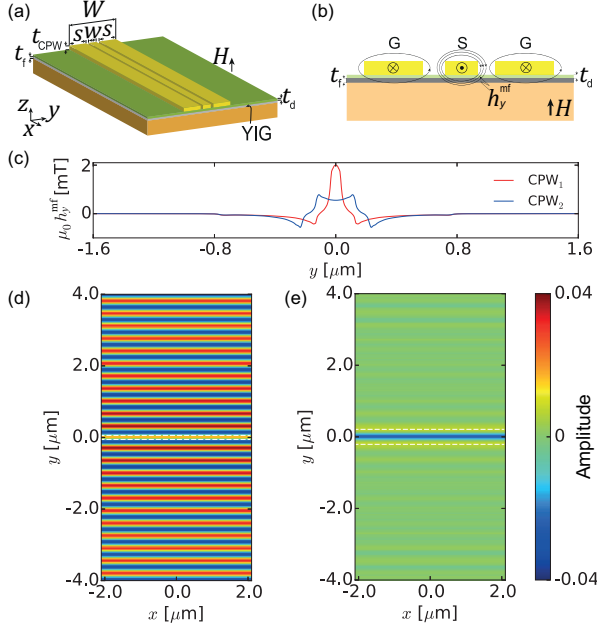


Figure 2. (a) Perspective view and (b) cross-section of a CPW consisting of a signal line (denoted by S) and two ground lines (denoted by G). A ferromagnetic (YIG) film of thickness t_f is separated from the CPW by a nonmagnetic, dielectric layer of thickness t_d . The YIG is saturated normal to the film plane by an external magnetic field H . The microwave signal transmitted along the x axis generates a magnetic field \mathbf{h}^{mf} , which exerts a torque on the magnetization in YIG. (c) The y component of the microwave magnetic field along the y axis, $h_y^{mf}(y)$, excited by CPW₁ (red line) and CPW₂ (blue line), obtained from CST simulations. (d)–(e) Dynamic component of the magnetization vector of the SWs induced by the microwave magnetic field from (d) CPW₁ and (e) CPW₂, obtained from MSs. The horizontal white dashed lines correspond to the signal line width.

$w_2 = 260$ nm. The total width of the transducers and the width of the gap between the signal and ground lines are the same in both waveguides: $W_1 = W_2 = 1.5$ μ m and $s_1 = s_2 = 85$ nm. By Fourier-transforming the field distributions from Fig. 2(c) we obtain the curves FT₁ and FT₂ from Fig. 1(b). This shows that the desired behavior of $h_y^{mf}(y)$ in the ferromagnetic film can be achieved by taking advantage of the sensitivity of the field profile of the CPW mode to the signal line width w . Indeed, Figs. 2(d) and 2(e) show the SWs induced by CPW₁ and CPW₂ at $f_0 = 22.12$ GHz, i.e., when $k_{SW}(f_0) \approx k_{exc}$ for the former and $k_{SW}(f_0) \neq k_{exc}$ ($k_{SW}(f_0) \approx k_{nexc}$) for the latter. Note that in CPW₂ $\mathcal{F}[h_{y,2}^{mf}(y)]$ is close to 0 at $k = k_{SW}(f_0)$, see Fig. 1(b). As expected, propagating SWs are excited only in CPW₁, in which Eq. (1) is satisfied.

To restrict SW generation to a short section of the transducer and hence to obtain a clearly defined beam, we vary the CPW geometry along the x axis. The signal line width is changed from w_2 at $x = -(l_w + l_b/2)$ to

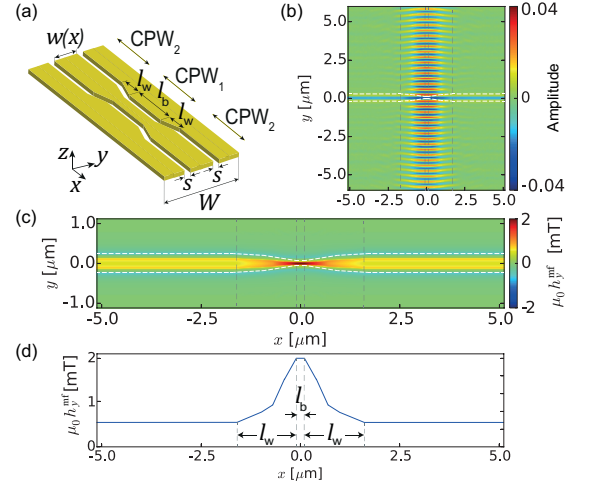


Figure 3. (a) Geometry of the nonuniform CPW proposed to excite an SW beam. (b) Dynamic component of the magnetization vector of the SW beam excited in a thin YIG film by the microwave magnetic field [shown in plot (c)] induced by the nonuniform CPW (results of MSs). (c) Distribution of the microwave magnetic field h_y^{mf} induced by the CPW on the top surface of the YIG film. The shape of the signal line is marked with dashed white lines. (d) Profile of h_y^{mf} along the axis of the signal line, $y = 0$.

w_1 at $x = -l_b/2$ and back from w_1 at $x = l_b/2$ to w_2 at $x = l_w + l_b/2$, as shown in Fig. 3(a). The gap width $s = 190$ nm and the total CPW width $W = 3$ μ m are kept constant. In calculations, we take $l_w = 1.5$ μ m and $l_b = 200$ nm. The microwave magnetic field distribution depends now also on the x coordinate: $h_y^{mf} = h_y^{mf}(x, y)$. To match the mesh cells of MSs, the field used in MSs was constructed by interpolating field profiles $h_y^{mf}(x_j, y)$ obtained from CST simulations at several values x_j of x (where $x_{j+1} - x_j = 150$ nm), using the following linear homotopic transformation providing a linear change of the line width between points x_j and x_{j+1} :

$$h_y^{mf}(x, y) = h_y^{mf}\left(x_j, y \frac{y_{0,j}}{B(x, y)}\right) + c(x) \left[h_y^{mf}\left(x_{j+1}, y \frac{y_{0,j+1}}{B(x, y)}\right) - h_y^{mf}\left(x_j, y \frac{y_{0,j}}{B(x, y)}\right) \right], \quad (3)$$

where $B(x, y) = y_{0,j} + c(x)(y_{0,j+1} - y_{0,j})$ and $c(x) = (x - x_j)/(x_{j+1} - x_j)$. The symbol $y_{0,j}$ denotes the zero of $h_y^{mf}(x_j, y)$ on the half-line $y > 0$. This approach was introduced to conserve the proper position of zeros of the field in the transition region. The map of the y component of the microwave magnetic field generated by this nonuniform CPW on the top surface of the ferromagnetic film is shown in Fig. 3(c).

Figure 3(d) shows the distribution of the dynamic magnetic field h_y^{mf} at the top surface of the YIG film along

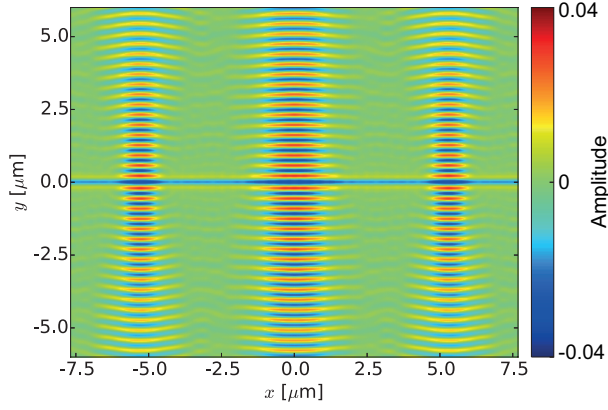


Figure 4. Dynamic component of the magnetization vector in three SW beams formed simultaneously in a thin YIG film by the microwave magnetic field generated by a single complex-shaped CPW (results of MSs). The left and right beams, generated by a nonuniform CPW with $l_b = 0$ nm and $l_w = 0.9$ μm , are narrower than the middle beam, generated by a CPW with $l_b = 100$ nm and $l_w = 1.8$ μm .

the x axis, i.e., the symmetry axis of the signal line. The dynamic component of the magnetization vector of a SW generated at 22.12 GHz with the aid of this CPW in the homogeneous YIG film is plotted in Fig. 3(b). The beam-type behavior of the SW is evident, so that the basic idea of the suggested approach is justified. As expected, the beam remains well convergent even at large distances from the transducer. The SW beam width at the half-power level is 1.5 μm in the beam waist lying at $y = 0$. This width can be controlled by adjusting the length of the transducer section having the profile of CPW₁, l_b , and the size and curvature of the transition section, l_w , as will be shown in the next paragraph. The minimum achievable beam width is likely to be restricted by the available nanofabrication technology.

Since the basic mechanism of SW beam generation in YIG films has now been numerically validated, it is worthwhile to consider further excitation scenarios. For example, multiple modulated sections can be introduced into a CPW to generate multiple coherent SW beams in a homogeneous ferromagnetic film. An example of SW excitation in a multibeam regime is presented in Fig. 4. As the beam divergence is weak, individual beams do not interfere with each other in the considered space region. Each beam may have different characteristics, such as its width and intensity, since they are determined by the geometry of the local CPW perturbation. This opens a route to multichannel structures for SWs created simply by modulating the microwave magnetic field through local modifications of the transducer geometry, with no need to make either the ferromagnetic film or the biasing magnetic field nonuniform.

The possibilities discussed above do not exhaust the broad range of potential applications of SW beam

magnonics. For instance, demultiplexer-type operation might be achieved by creating such a distribution of $h_y^{\text{mf}}(x, y)$ that injection of a mixed dual-frequency microwave signal into the CPW would cause efficient generation of SW beams at two distinct frequencies within different regions of the YIG film, associated with different virtual propagation channels. However, to realize this regime, additional design efforts are required, e.g., to limit excitation at undesirable frequencies in both channels.

SW beams can also be utilized for sensing, transmitting signals, or performing logic operations. In particular, the concepts of logic elements based on interference effects, such as Mach-Zehnder interferometers, can also be adapted for SW-beam-based operation, provided that a mechanism for introducing a controllable phase shift between two SW beams is developed. Reading can be done by direct beam interference [31] (this will require a change of the beam propagation direction) or using a detecting CPW transducer of appropriate width [32, 33].

To summarize, we have proposed to use nonuniform microwave CPW transducers to excite effectively even high frequency SW beams in thin YIG films. Modulation of the transducer geometry ensures that the necessary condition of SW generation, the match between the SW wave vector and the maximum of the spatial Fourier transform of the microwave magnetic field induced by the transducer, is satisfied only locally, in a short section of the waveguide. The beam characteristics, such as its waist width, are controlled by the geometry of the modulated transducer section. The presented numerical examples demonstrate the potential of the proposed approach, which holds promise as a platform for future SW-based circuitry. In particular, we have shown that multiple SW beams associated with separate virtual propagation channels can be generated in a single thin ferromagnetic film. Manipulation of such beams in particular magnonic devices will be the subject of upcoming research.

The research received funding from the National Science Center of Poland UMO-2012/07/E/ST3/00538 and from the European Union Horizon 2020 research and innovation programme under the Marie Skłodowska-Curie grant agreement No 644348. Part of the calculations presented in this paper was performed at the Poznan Supercomputing and Networking Center. AES thanks his colleagues from the Bilkent University, Ankara, for help with CST simulations. PG would like to thank L. Nizio for fruitful discussions.

* pawel.gruszecki@amu.edu.pl

† krawczyk@amu.edu.pl

- [1] V. V. Kruglyak, S. O. Demokritov, and D. Grundler, J. Phys. D: Appl. Phys. **43**, 264001 (2010).
- [2] V. E. Demidov, M. P. Kostylev, K. Rott, P. Krzysieczko,

- G. Reiss, and S. O. Demokritov, *Appl. Phys. Lett.* **95**, 112509 (2009).
- [3] Y. Au, M. Dvornik, T. Davison, E. Ahmad, P. S. Keatley, A. Vansteenkiste, B. Van Waeyenberge, and V.V. Kruglyak, *Phys. Rev. Lett.* **110**, 097201 (2013).
- [4] Y. Kajiwara, K. Harii, S. Takahashi, J. Ohe, K. Uchida, M. Mizuguchi, H. Umezawa, H. Kawai, K. Ando, K. Takanashi, S. Maekawa, and E. Saitoh, *Nature* **464**, 262 (2010).
- [5] K. Vogt, F. Y. Fradin, J. E. Pearson, T. Sebastian, S. D. Bader, B. Hillebrands, A. Hoffmann, and H. Schultheiss, *Nat. Commun.* **5**, 3727 (2014).
- [6] S. Klingler, P. Pirro, T. Bracher, B. Leven, B. Hillebrands, and A. V. Chumak, *Appl. Phys. Lett.* **105**, 152410 (2014).
- [7] T. Bracher, F. Heussner, P. Pirro, T. Fischer, M. Geilen, B. Heinz, B. Lagel, A. A. Serga, and B. Hillebrands, *Appl. Phys. Lett.* **105**, 232409 (2014).
- [8] V. Vlaminck and M. Bailleul, *Science* **322**, 410 (2008).
- [9] K. Bernstein, R. K. Cavin, W. Porod, A. Seabaugh, and J. Welser, *Proc. IEEE* **98**, 2169 (2010).
- [10] D. E. Nikonov and I. A. Young, *Proc. IEEE* **101**, 2498 (2013).
- [11] T. An, et al., *Nature Mat.* **12**, 549 (2013).
- [12] M. Madami, S. Bonetti, G. Consolo, S. Tacchi, G. Carlotti, G. Gubbiotti, F. B. Mancoff, M. A. Yar, and J. Akerman, *Nat. Nanotechnol.* **6**, 635 (2011).
- [13] M. Krawczyk and D. Grundler, *J. Phys. Cond. Matter* **26**, 123202 (2014).
- [14] M. Mruczkiewicz, M. Krawczyk, R. V. Mikhaylovskiy, and V. V. Kruglyak, *Phys. Rev. B* **86**, 024425 (2012).
- [15] V. E. Demidov, O. Dzyapko, M. Buchmeier, T. Stockhoff, G. Schmitz, G. A. Melkov, and S. O. Demokritov, *Phys. Rev. Lett.* **101**, 257201 (2008).
- [16] T. Schneider, A. A. Serga, A. V. Chumak, C. W. Sandweg, S. Trudel, S. Wolff, M. P. Kostylev, V. S. Tiberkevich, A. N. Slavin, and B. Hillebrands, *Phys. Rev. Lett.* **104**, 197203 (2010).
- [17] J. W. Boyle, S. A. Nikitov, A. D. Boardman, J. G. Booth, and K. Booth, *Phys. Rev. B* **53**, 12173 (1996).
- [18] M. Bauer, et al., *Phys. Rev. B* **56**, R8483 (1997).
- [19] M. Bini, L. Millanta, and N. Rubino, *J. Appl. Phys.* **46**, 3175 (1975).
- [20] V. Vlaminck and M. Bailleul, *Phys. Rev. B* **81**, 014425 (2010).
- [21] I. S. Maksymov and M. Kostylev, *Physica E* **69**, 253 (2015).
- [22] See www.cst.com.
- [23] A. Vansteenkiste, J. Leliaert, M. Dvornik, M. Helsen, F. Garcia-Sanchez, and B. Van Waeyenberge, *AIP Adv.* **4**, 107133 (2014).
- [24] Y. Sun, Y.-Y. Song, H. Chang, M. Kabatek, M. Jantz, W. Schneider, M. Wu, H. Schultheiss, and A. Hoffmann, *Appl. Phys. Lett.* **101**, 152405 (2012).
- [25] H. Yu, O. d'Allivy Kelly, V. Cros, R. Bernard, P. Bortolotti, A. Anane, F. Brandl, R. Huber, I. Stasinopoulos, and D. Grundler, *Sci. Rep.* **4**, 6848 (2014).
- [26] D. Stancil and A. Prabhakar, *Spin Waves: Theory and Applications*, (Springer, 2009).
- [27] The MSs were performed for the structure shown in Fig. 2. The simulated structures were large enough to prevent boundary effects from having a significant influence on SW dynamics in the central part of the film. Moreover, absorbing boundaries were introduced at the edges of the computational domain parallel to the transducer axis (i.e., at $|y| = L_y/2$, where L_y is the size of the computational domain in the y direction); see the supplementary material to [28]. In addition, periodic boundary conditions were applied on the edges perpendicular to the transducer axis (i.e., at $|x| = L_x/2$, where L_x is the size of the computational domain in the x direction) to avoid the effects of abrupt symmetry breaking of the dynamic magnetic field.
- [28] P. Gruszecki, J. Romero-Vivas, Yu. S. Dadoenkova, N. N. Dadoenkova, I. L. Lyubchanskii, and M. Krawczyk, *Appl. Phys. Lett.* **105**, 242406 (2014).
- [29] This frequency is achievable by standard microwave generators, and at this frequency the dispersion relation of SWs in YIG thin film is almost isotropic also when the magnetization saturation is in-plane of the film. This makes the results of our paper more general. However, at small enough wave vectors the strong anisotropy of the dispersion relation has to be taken into account.
- [30] C. Kittel, *Introduction to Solid State Physics*, (John Wiley & Sons, Inc. 1996).
- [31] R. Hertel, W. Wulfhchel, and J. Kirschner, *Phys. Rev. Lett.* **93**, 257202 (2004).
- [32] T. Schneider, A. A. Serga, B. Leven, B. Hillebrands, R. L. Stamps, and M. P. Kostylev, *Appl. Phys. Lett.* **92**, 022505 (2008).
- [33] N. Sato, K. Sekiguchi, and Y. Nozaki, *Appl. Phys. Express* **6**, 063001 (2013).
- [34] J. R. Dormand, P. J. Prince, *J. Comp. Appl. Math.* **6**, 19 (1980).